Modeling Endpoint Distribution of Pointing Selection Tasks in Virtual Reality Environments

DIFENG YU, The University of Melbourne, Australia and Xi'an Jiaotong-Liverpool University, China
HAI-NING LIANG*, Xi'an Jiaotong-Liverpool University, China
XUESHI LU, Xi'an Jiaotong-Liverpool University, China
KAIXUAN FAN, Xi'an Jiaotong-Liverpool University, China
BARRETT ENS, Monash University, Australia

Understanding the endpoint distribution of pointing selection tasks can reveal the underlying patterns on how users tend to acquire a target, which is one of the most essential and pervasive tasks in interactive systems. It could further aid designers to create new graphical user interfaces and interaction techniques that are optimized for accuracy, efficiency, and ease of use. Previous research has explored the modeling of endpoint distribution outside of virtual reality (VR) systems that have shown to be useful in predicting selection accuracy and guide the design of new interactive techniques. This work aims at developing an endpoint distribution of selection tasks for VR systems which has resulted in *EDModel*, a novel model that can be used to predict endpoint distribution of pointing selection tasks in VR environments. The development of EDModel is based on two users studies that have explored how factors such as target size, movement amplitude, and target depth affect the endpoint distribution. The model is built from the collected data and its generalizability is subsequently tested in complex scenarios with more relaxed conditions. Three applications of EDModel inspired by previous research are evaluated to show the broad applicability and usefulness of the model: correcting the bias in Fitts's law, predicting selection accuracy, and enhancing pointing selection techniques. Overall, EDModel can achieve high prediction accuracy and can be adapted to different types of applications in VR.

CCS Concepts: • **Human-centered computing** → **HCI theory, concepts and models**; *Pointing*; User studies; • **Computing methodologies** → *Virtual reality*.

Additional Key Words and Phrases: target selection, selection modeling, endpoint distribution, Fitts's Law, error prediction

ACM Reference Format:
Difeng Yu, Hai-Ning Liang, Xueshi Lu, Kaixuan Fan, and Barrett Ens. 2019. Modeling Endpoint Distribution of Pointing Selection Tasks in Virtual Reality Environments. *ACM Trans. Graph.* 38, 6, Article 218 (November 2019), 13 pages. https://doi.org/10.1145/3355089.3356544

*Corresponding author who can be contacted via haining.liang@xjtlu.edu.cn

Authors' addresses: Difeng Yu, difeng.yu@student.unimelb.edu.au, The University of Melbourne, Australia, Xi'an Jiaotong-Liverpool University, China; Hai-Ning Liang, haining.liang@xjtlu.edu.cn, Xi'an Jiaotong-Liverpool University, China; Xueshi Lu, xueshi.lu17@student.xjtlu.edu.cn, Xi'an Jiaotong-Liverpool University, China; Kaixuan Fan, kaixuan.fan16@student.xjtlu.edu.cn, Xi'an Jiaotong-Liverpool University, China; Barrett Ens, barrett.ens@monash.edu, Monash University, Australia.

0730-0301/2019/11-ART218 $15.00
https://doi.org/10.1145/3355089.3356544

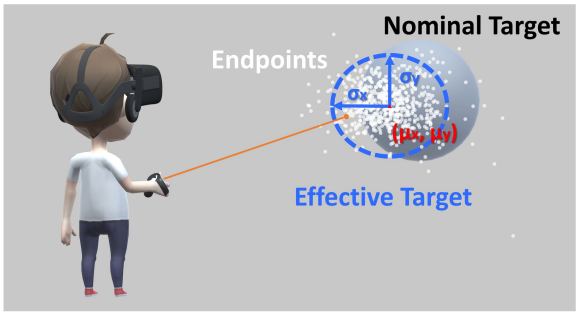

Fig. 1. The effective target calculated from selection endpoints might not be the same as the nominal target. EDModel is based on the bivariate-Gaussian distribution $\mathcal{N}_2(\boldsymbol{\mu}, \Sigma)$ and can predict how endpoints are distributed when selecting targets with different characteristics (width, distance, and depth) in virtual reality environments.

1 INTRODUCTION

One of the primary and most common tasks in current interactive virtual reality (VR) systems is target selection of menus and buttons or other objects. Virtual pointing techniques like raycasting allow users to select targets beyond their area of reach with relatively little physical movement. Raycasting has been extensively used in current consumer VR systems like Oculus RIFT and HTC VIVE and in a wide range of applications and games. Despite their prevalence, flexibility, and usefulness, virtual pointing techniques typically suffer severely when targets are small, far away from users, or occluded by other elements within the virtual reality environment (VE) [Argelaguet and Andujar 2013]. As a result, the design of 3D graphical user interfaces and new interactive techniques that support efficient, accurate, and effortless target selection in VEs is still challenging.

Research on pointing selection tasks in VE can be broadly classified into two groups: (1) adding enhancements to interactive techniques, and (2) building models. Enhancement techniques (e.g., [Bowman et al. 2004; Tu et al. 2019]) incorporate additional features to support fast and precise selection. For example, a recent publication [Baloup et al. 2019] has presented RayCursor which aims to enable precise selection by filtering noisy inputs and embedding a movable pointer (along the depth axis) on the ray. Some other research has applied or built user performance models for 3D virtual space to aid user interface (UI) design decisions. Most of these models are based on Fitts's law [Argelaguet and Andujar 2009; Kopper et al. 2010; Qian and Teather 2017; Wingrave and Bowman

2005]. Our review of the literature shows that there is little work in VR on modeling the endpoint distribution of pointing selection tasks, which is the probability of the pointing ray being in a certain position and orientation when a selection is triggered. Our paper focuses on filling this gap.

Unlike Fitts's law, which only accounts for movement time, modeling the endpoint distribution allows us to uncover the underlying source(s) of selection errors and uncertainties according to the important characteristics of targets [Huang et al. 2018; Wobbrock et al. 2008]. It can also provide us with insights on how users actually acquire a given target, probably without considering about its nominal size [Crossman 1957; Zhai et al. 2004] (see Figure 1). Further, a useful model of endpoint distribution can allow us to predict the possible selection points or areas based on the characteristics of the target (such as target width and distance); as such, it can help in the design and framing of new UI and novel interactive techniques that allow accurate, efficient, and easy selection of targets [Grossman and Balakrishnan 2005; Grossman et al. 2007; Li et al. 2018].

In this paper, we introduce EDModel, a novel endpoint distribution model developed from empirical data of pointing selection tasks in VE. We present two user studies which have explored how different factors (such as target size, movement amplitude, and target depth) affect the endpoint distribution and how these effects can be modeled. We further propose three applications of EDModel inspired by past research to aid designers of new 3D UI and interactive techniques that aim to improve users' pointing selection performance. We illustrate the study limitations and point out future working directions, and provide a conclusion at the end.

In this paper, we make four main contributions:

- EDModel: an endpoint distribution model based on bivariate-Gaussian distribution in both simple and complex scenarios for pointing selection tasks in VEs.
- Two user studies that model pointing selection distribution in VEs and provide insights on how different factors (such as target width, movement amplitude, and target depth) might affect the endpoint distribution, as summarized in Section 5.
- Three applications of EDModel inspired by previous research: (1) correcting the bias in Fitts's Law, (2) predicting selection accuracy, and (3) BayesPointer (a selection enhancement technique) for pointing selection in VR, as demonstrated in Section 6.
- An open-source dataset that includes 20640 pointing selection trials in VR collected in Study 1 and Study 2, and also the data processing scripts for replication and future research (see Appendix A for details).

2 RELATED WORK

In this section, we review and summarize related work regarding pointing selection in VR, endpoint deviation and its causes, and modeling endpoint distribution.

2.1 Pointing Selection in VR

Pointing selection is one of the main metaphors for acquiring targets in current VR systems [Argelaguet and Andujar 2013]. The most common technique allows a user to point at an object with a virtual ray which defines the pointing direction. The closest object that intersects with the ray can be selected by pressing the selection trigger. The virtual ray can either emanate from the user's hand position (hand-based pointing) or from the tracked head position (head-based pointing) [Bowman et al. 2004]. Despite the extensive use of this technique, pointing selection is notoriously difficult for acquiring small or distant targets (cf. [Argelaguet and Andujar 2013]).

To overcome the selection difficulty, some researchers have proposed enhancement techniques for efficient object selection (for example, [Baloup et al. 2019; Tu et al. 2019; Vanacken et al. 2007]). Others have explored models of how people perform pointing and selection tasks to allow for a better understanding of the process and further make reliable performance predictions [Kopper et al. 2010; Wingrave and Bowman 2005]. However, most of the research on modeling pointing selection in VR is about movement time estimation based on Fitts's law [Fitts 1954; Soukoreff and MacKenzie 2004]. Hence, we still do not know much about the underlying properties of how selection endpoints actually are distributed.

2.2 Endpoint Deviation and Speed-Accuracy Tradeoff

Past research (e.g., [Wobbrock et al. 2011b]) has distinguished between two sources of selection errors: constant and variable. The constant error is defined as the mean distance of endpoints to the target center, whereas the variable error reflects the spread of hits, or endpoint deviation.

The endpoint deviation is usually determined by different speed-accuracy biases of users who might factor in how costly an error is when a making selection [Banovic et al. 2013; Zhai et al. 2004]. Since there is already extensive research related to speed-accuracy tradeoff, we direct interested readers to literature reviews in [Plamondon and Alimi 1997; Wobbrock et al. 2008] and some more recent publications [Guiard et al. 2011; Guiard and Rioul 2015; MacKenzie and Isokoski 2008]. When influenced by the tradeoff, a user may or may not comply with the precision required by a task, and this could lead the endpoint dispersion to depart from the target area [Schmidt et al. 1979; Zhai et al. 2004]. In other words, a more "aggressive" user, for example, who might select the target in a breakneck speed could lead to a low selection accuracy with large endpoint dispersion. In contrast, a more cautious user, who might slow down the pace to achieve higher accuracy, tends to have a smaller deviation of selection endpoints. Some studies [Banovic et al. 2013; Soukoreff and MacKenzie 2009] indicate that users are likely to favor efficiency and lean towards optimal speed-accuracy tradeoff, which could minimize the task completion time.

While speed-accuracy tradeoff might vary for different users, some researchers have been trying to explore how users will typically behave by modeling the endpoint distribution in selection tasks.

2.3 Endpoint Distribution Modeling

There has been long interest in exploring the distribution of selection endpoints. In 1968, Welford observed that the endpoint deviation in a 1D task followed a Gaussian distribution [Welford 1968]. Later, results from Schmidt et al.'s studies [Schmidt et al. 1979] indicated that the errors that are parallel and perpendicular to the movement

direction could probably produce an elliptical distribution, with the long axis in line with the direction of movement. Similarly, setting the target to a fixed angle (45°), Murata [1999] noticed that the distribution of the horizontal and vertical coordinates of endpoints could be approximated by the Gaussian distribution.

More recently, Grossman and Balakrishnan [2005] built a probabilistic model for 2D rapid pointing tasks. Their model assumes that the spread of hits would follow a bivariate normal distribution. The model calculated the probability of hitting a target by integrating the distribution and further mapped the probability to an index of difficulty (*ID*) value. The model was shown to have a good level of prediction for movement time. By varying distances and angles of movement, Grossman and Balakrishnan also found that the distribution for selecting square targets has a larger spread (twice as large) in the direction of movement than in the direction perpendicular to the movement regardless of movement angles. Also, they found that the deviations in both directions increased with the target distance by a constant factor. Grossman et al. [2007] further generalized their model to targets with arbitrary shapes.

Bi and colleagues conducted a series of experiments to investigate the distribution of endpoints for finger touch input. Bi et al. [2013] first proposed a dual-distribution hypothesis, which assumed the endpoint distribution came from two independent normal distributions—one governed by the speed-accuracy tradeoff and the other reflected the absolute precision of finger touch. They then derived the FFitts Law for predicting finger touch performance based on endpoint distribution. Later, Bi and Zhai [2013] combined Bayes' theorem with the dual-distribution hypothesis to improve target selection accuracy. Their study indicated a strong linear relationship between endpoint variance and target size. Bi and Zhai [2016] further developed a model to predict selection accuracy inspired by how selection endpoint distributes. Recent work by Yamanaka [2018a,b] showed that FFitts Law could not be applied when the absolute deviation was larger than the total distribution. In contrast to the approaches based on the dual-distribution hypothesis, our work models the whole distribution directly (more on this later).

Several other researchers have studied endpoint distribution in selection tasks that involve moving targets instead of stationary ones. Huang et al. [2018] found a Ternary-Gaussian model for moving target selection in 1D. Li et al. [2018] further extended the Ternary-Gaussian model to a 2D context. Lee and colleagues [Huang and Lee 2019; Lee et al. 2018; Lee and Oulasvirta 2016; Lee et al. 2019; Park et al. 2018] have also been working on endpoint distribution modeling for moving target selection that considers the internal mechanisms by which a user interacts with a computer. Apart from target selection, endpoint distribution has also been modeled for reducing noisy input in text entry tasks [Goodman et al. 2002; Yu et al. 2017].

This current work differs from existing research in several ways. First, our work is for VR environments, while previous work focused on other types of displays and devices. VR poses extra challenges because users are fully immersed in the 3D VE and could interact with targets located in different places and depths. Current VR systems also use unique and different input paradigms comparing to traditional mouse and stylus input. For example, the most popular VR systems like the Oculus RIFT and HTC Vive allow head-pointing via the head-mounted display (HMD) or hand-pointing via their dual-handheld controllers. In addition, while previous work modeled the endpoint distribution based on strong assumptions, our model is derived from empirical data from two user experiments. Besides, we have considered extreme conditions to test the generalizability of our model, while most previous works have not taken into account these conditions. Finally, we also released the collected dataset for replication and to support future work.

3 STUDY 1

One purpose of this first study was to verify whether the endpoint distribution of pointing selection in VEs follows the bivariate-Gaussian distribution[1]. We also aimed to explore the effects (and possible interaction effects) of target width W and movement amplitude A on the endpoint distribution. We were further interested in predicting the parameters of the bivariate-Gaussian distribution, specifically the mean vector $\boldsymbol{\mu}$ and the covariance matrix Σ (see Equation 1), through the influential factors.

$$\boldsymbol{X} \sim \mathcal{N}_2(\boldsymbol{\mu}, \Sigma) \tag{1}$$

3.1 Hypotheses

Based on the past literature and our pilot results, we formulated the following hypotheses before the study:

- ***H1***. *The endpoint distribution of pointing selection in VEs is bivariate-Gaussian.* Previous studies have indicated or hypothesized that the endpoint distribution of 2D pointing selection could be bivariate-Gaussian for finger touch-based input [Bi et al. 2013; Bi and Zhai 2013; Wang and Ren 2009] and puck-tablet interface [Grossman and Balakrishnan 2005]. Our pilot results also suggested that this hypothesis could hold for pointing selection in VR.
- ***H2***. *The target width W affects the endpoint distribution significantly.* Previous findings suggested that there were strong linear relationships between the standard deviation of the Gaussian distribution and the target width when selecting 2D circular targets with finger touch [Bi and Zhai 2013]. Our pilot results indicated that it could also be true for pointing selection in VR.
- ***H3***. *The movement amplitude A does not affect the endpoint distribution in a significant way.* Bi and Zhai have suggested in their work that the endpoint distribution for selecting 2D circular targets using finger touch was solely specified by the target size W (and not movement amplitude A) [Bi and Zhai 2013]. Recent work in selecting 1D moving targets suggested that the initial distance A does not affect the endpoint distribution [Huang et al. 2018]. In contrast, Grossman and Balakrishnan have found that the spread of hits (standard deviations of the Gaussian distribution) increased by a constant factor with A [Grossman and Balakrishnan 2005]. Despite this inconsistency found in the past literature, we here hypothesized that the movement amplitude A would not affect the endpoint distribution significantly.
- ***H4***. *There is no interaction effect of target width W and movement amplitude A on the endpoint distribution.* Past research did not consider the interaction effect of target width W and movement

[1] A simple introduction to the bivariate-Gaussian distribution necessary for this research is provided in Appendix B.

amplitude A on endpoint distribution. We hypothesized that there would be no interaction effect between W and A.

3.2 Participants, Apparatus, and Materials

Sixteen participants (6 females, 10 males) between the ages of 19-27 (mean = 21) were recruited from a local university campus. Data from the pre-experiment questionnaire showed that twelve of them had at least some VR experience before. They all had a normal or corrected-to-normal vision.

We used an Oculus RIFT CV1 headset, which had 1080 × 1200 screen resolution per eye and an around 110° diagonal field-of-view (FoV), to completely immerse the users into the 3D VE. A pair of Oculus Touch wireless controllers were used as the input device. The experiment was conducted on an Intel Core i7 processor PC with a dedicated NVIDIA GTX 1080 Ti graphics card. The program was developed using C#.NET and was run on the Unity3D platform.

3.3 Experimental Task and Measurements

The experimental task was designed similar to ISO9241-9 multi-directional tapping task [ISO 2000; Soukoreff and MacKenzie 2004] for head pointing selection with 21 spherical targets on the Fitts's ring (see Figure 2A). The participants were required to select the targets in a clockwise manner, following the path indicated in Figure 2B. For each trial, a participant needed to move the cursor, which was always at the center of the FoV, to the highlighted goal target and click the trigger of the controller to confirm the selection. After the selection was made, a short sound was provided and the next trial would start with a new goal target highlighted. The participant then had to move the cursor to the new goal target. No feedback was provided to indicate the correctness of the selection. The selection mechanism was chosen to be head-based pointing, as it could be used in VR systems with or without a handheld controller.

We varied two independent variables in this experiment: target width W and movement amplitude A (see Figure 2A). The two variables were described in the angular form [Kopper et al. 2010; Petford et al. 2018]. That is, the subtended angles of W and A were calculated from the viewpoint of each participant and were used to determine the different levels of the variables. According to our setting, the radius of the target ring R is approximate to half of A (i.e., $2R \approx A$).

As we were using angular representation, it could be easier to use a spherical coordinate system (r, θ, φ), where two angles (θ and φ) and one distance (r) were used to define a point in 3D (see [ISO 2009]). Since the pointing ray which was emitted from the pointing device can be seen to have an infinite length, we can further simplify the point representation to a 2D coordinate (by ignoring r) in this experiment. Therefore, we defined an endpoint $p = (x, y)$: x as the angular error distance parallel to the direction of movement (from the starting target to the goal target), y is the angular error distance perpendicular to the line of movement (as shown in Figure 2C). Both x and y can have negative values. The origin of the two axes was set at the center of the goal target.

3.4 Design and Procedure

The study used a 8×3 within-subjects design with two factors: target width W (1° to 4.5°, with an increment step of 0.5°) and movement amplitude A (30°, 35°, and 40°). The values were determined by preliminary tests and we ensured in the extreme condition (W=4.5° and A=30°), the targets on the Fitts's ring would not occlude each other. The distance between the user and each target was a constant value (100m). The order of the W was counterbalanced using the Latin Square approach. For a given W, the three A conditions were presented in random order. For each $W \times A$ combination (one ring), the first trial was discarded, leaving 20 timed repetitions. In sum, we collected 7680 endpoints (8 W × 3 A × 16 participants × 20 repetitions) from the experiment.

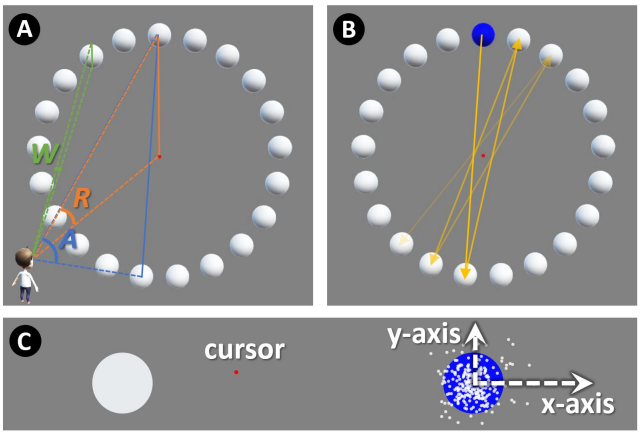

Fig. 2. (A) The angular form of target width W, movement amplitude A, and the radius of the Fitts's ring R. (B) The user followed the path indicated by the arrows to select the targets sequentially. (C) The x-axis was defined as the direction of movement, while the y-axis was perpendicular to the line of movement. The origin was set at the center of the goal target.

The whole study lasted about fifteen minutes for each participant. The workload of this continuous selection task was designed to be relatively low, since the tiredness of using the VR device could potentially influence the final results. Before the experiment, we first invited the participants to fill in a questionnaire to gather their demographic information. They were then introduced to the VR device and the selection task. After that, they wore the VR headset and started the practice trials. They also calibrated their head positions to the origin of the VR environment. Next, they proceeded to the formal trials. They were instructed to select the target naturally, rather than maintaining a 4% error rate as in many other studies. Any speed-accuracy instructions will strongly modulate the endpoint spreads [Guiard et al. 2011], despite the fact that some users would still tend to perform the tasks with their own strategies [Zhai et al. 2004]. In this experiment, we wanted to simulate how users would perform the selection in a natural way where they could control their own pace to complete each task rather than following potentially unnatural instructions. During the formal experiment, participants did not take any breaks.

3.5 Data Pre-processing

As a common practice (e.g., [Huang et al. 2018]), we removed the outliers that deviated by more than three standard deviations from (1) the averaged center of both axes and (2) the averaged movement

Table 1. The results of RM-ANOVAs in Study 1.

Factor	*DV**	df_{effect}	df_{error}	F	p	η_p^2	Sig?
W	μ_x	3.659	54.889	2.330	.073	.134	no
A	μ_x	1.689	25.332	11.722	.000	.439	**yes**
$W \times A$	μ_x	6.934	104.008	1.698	.118	.102	no
W	σ_x	3.758	56.373	58.587	.000	.796	**yes**
A	σ_x	1.924	28.861	0.608	.545	.039	no
$W \times A$	σ_x	6.002	90.036	0.892	.505	.056	no
W	μ_y	4.923	73.845	0.760	.579	.048	no
A	μ_y	1.801	27.019	0.991	.337	.062	no
$W \times A$	μ_y	5.690	85.352	0.740	.612	.047	no
W	σ_y	3.226	48.392	49.013	.000	.766	**yes**
A	σ_y	2.000	29.999	0.652	.528	.042	no
$W \times A$	σ_y	6.495	97.428	0.908	.498	.057	no
W	ρ	4.503	67.542	0.631	.661	.040	no
A	ρ	1.765	26.476	0.154	.832	.010	no
$W \times A$	ρ	7.144	107.158	0.775	.612	.049	no

*Dependent variable (DV) ⋆Significant level α: 0.05

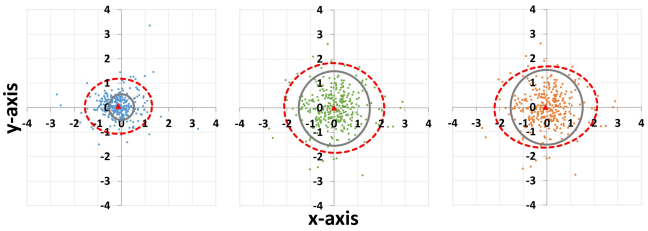

Fig. 3. Distributions of endpoints across all participants in 3 sample sets (left): $W = 1°$, $A = 30°$ (middle): $W = 3°$, $A = 30°$ (right): $W = 3°$, $A = 40°$. The grey circles are the targets, while the red dashed ellipses are 95% confidence ellipses.

time within each $A \times W$ condition. According to previous research, these "accidental clicks" could be induced by confusion of the participants [Zhai et al. 2004]. In addition, we found that when making a selection, some participants misclicked the trigger twice which "skipped" one trial in the middle and caused the endpoint to be very far from the target position. Therefore, a total of 262 trials (3.41%) were discarded, leaving 7418 trials. The endpoints were grouped into 384 sets (24 conditions × 16 participants) for analysis. Figure 3 shows three sample sets of endpoint distributions.

3.6 Results

All sets of endpoints passed the Kolmogorov-Smirnov test provided by MATLAB (`kstest()`) for normality of distribution in both x- and y axes ($\alpha = 0.05$) . We then estimated the mean μ and the standard deviation σ of the Gaussian distribution using the maximum likelihood estimates (MLEs, `mle()` in MATLAB) for each set in both axes. The correlation ρ between the two axes was calculated through the function `corrcoef()`. Therefore, for each set of endpoints, we were able to calculate the mean vector $\boldsymbol{\mu}$ and the covariance matrix Σ

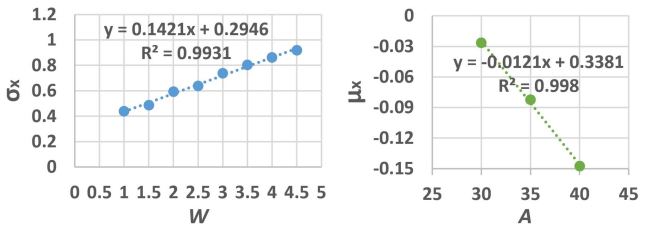

Fig. 4. Averaged σ_x of subjects' endpoint distributions for eight levels of W (left) and averaged μ_x for three levels of A (right). The regression indicated strong linear relationships between the factors and their corresponding dependent variables.

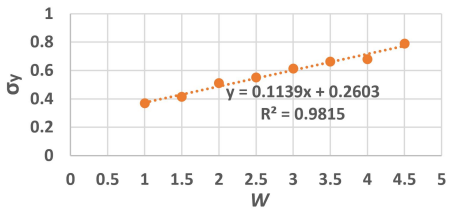

Fig. 5. Averaged σ_y of subjects' endpoint distributions for eight levels of W. The regression indicated a strong linear relationship.

with five dependent variables μ_x, σ_x, μ_y, σ_y, and ρ (see Equation 19 in Appendix B for details).

The results from repeated-measures ANOVA (RM-ANOVA) of the five dependent variables (*DV* for short) are summarized in Table 1. The degree of freedom was adjusted by the Greenhouse-Geisser correction for violation of sphericity. W was shown to have a significant main effect on both σ_x and σ_y; while A had a significant main effect on μ_x. No other effects or interactions were found. The mean values of μ_y and ρ which were not significantly affected by both W and A were calculated to be 0.033 (s.e. = 0.007) and -0.022 (s.e. = 0.013) respectively across all sets of endpoints.

The linear regressions were conducted on the factors that had main effects on the dependent variables. As shown in Figure 4-5, the regression indicated strong linear relationships between W with σ_x ($R^2 = 0.99$), W with σ_y ($R^2 = 0.98$), and A with μ_x ($R^2 = 1.00$). They also showed non-zero intercepts on the y-axis. The estimated linear relationships were: $\sigma_x = 0.1421W + 0.2946$, $\mu_x = -0.0121A + 0.3381$, and $\sigma_y = 0.1139W + 0.2603$.

3.7 Discussion

Our results indicate that ***H1*** could be valid since (1) all sets of endpoints passed the normality test in both x- and y-axis—i.e., **X** and **Y** are both normally distributed, and (2) it is probably reasonable to assume that the two variables **X** and **Y** are independent as the occurrence of either one of them is unlikely to affect the probability of occurrence of the other. Therefore, our data suggest that the endpoint distribution of pointing selection in VEs probably, and likely, follow a bivariate-Gaussian function.

Our ***H2*** is supported—the RM-ANOVA indicate statistical main effects of W on both σ_x and σ_y. The regression also reveals strong linear relationships of W on both dependent variables. This finding

is consistent with previous research in non-VR environments [Bi and Zhai 2013]. From the estimated linear relationship $\sigma_x = 0.1421W + 0.2946$ and $\sigma_y = 0.1139W + 0.2603$, we can see non-zero intercepts (about 0.3) on both σ_x and σ_y. This indicates that when the target width becomes zero, there is probably an unavoidable selection variance on both axes.

Our ***H3*** is not supported—the RM-ANOVA suggest a statistical main effect of A on μ_x. The regression shows a strong linear relationship $\mu_x = -0.0121A + 0.3381$. The relationship shows that the participants became a bit "lazy" for selecting further targets (an increased required movement amplitude led to a decreased relative actual movement). This is inconsistent with previous findings, as A neither has zero effect on the endpoint distribution as indicated in Bi and Zhai's work [Bi and Zhai 2013] nor has an effect on standard deviations σ as demonstrated in Grossman and Balakrishnan's research [Grossman and Balakrishnan 2005]. The regression indicates an extremely strong fit ($R^2 = 1.00$). However, we have to be cautious because (1) since we had envisioned no effect of A, we tested only 3 levels of A which might be somewhat small to confirm this linear relationship, and (2) the intercept of μ_x is not zero which was somewhat against our intuition—intuitively, in the static pointing scenario (movement amplitude A = 0), the mean value should be in the center ($\mu_x = 0$). Moreover, this "lazy effect" could come from an increased R, rather than an increased A, as the muscle might constrain the movement and thus make the users become "lazy". With an ISO9241-9 task setting, we could not verify which sources the effect came from. As a result, further investigation was still needed based on other tasks.

Our results suggest that there is no interaction effect of W and A on the endpoint distribution, supporting our ***H4***.

Apart from verifying the hypotheses, the results also reveal some other important findings. Our results suggest that the correlation coefficient ρ between X and Y will not be affected by either W or A and is nearly equals to zero (ρ = -0.022). That is, there is no correlation between X and Y, confirming the assumptions made by [Bi and Zhai 2013; Grossman and Balakrishnan 2005]. Similarly, μ_y is approximately zero ($\mu_y = 0.033$) which shows that the endpoints distribute around the center of the y-axis. In addition, we need to be cautious against using the hardbound ($\alpha = 0.05$) to determine if one factor will have a significant main effect on the distribution. Our results suggest that W and $W \times A$ could possibly have an effect on μ_x (p = .073 and p = .118, respectively), both with a medium level of effective size. However, for the simplicity of the model, these factors were not taken into consideration when building the model, as they did not show a clear (or strong enough) effect.

According to the results of this first study, we have been able to create the bivariate-Gaussian distribution model for pointing selection tasks in VR with the following parameters:

$$\boldsymbol{\mu} = \begin{bmatrix} eA + f \\ 0 \end{bmatrix}, \Sigma = \begin{bmatrix} (aW + b)^2 & 0 \\ 0 & (cW + d)^2 \end{bmatrix} \quad (2)$$

where our data suggest that $a = 0.1421$, $b = 0.2946$, $c = 0.1139$, $d = 0.2603$, $e = -0.0121$, and $f = 0.3381$. For ease of reference, we name the endpoint distribution model determined by the study for pointing selection in virtual reality environments as *EDModel*.

Based on the discussion above, we still need to verify how μ_x is actually affected by the movement amplitude A. Moreover, it is important to see if our model could be generalized to more complex VR scenarios.

4 STUDY 2

This study aimed to test the robustness and reliability of EDModel by increasing the complexity of the pointing selection task in VR environments. As an essential 3D feature, the visual depth of the target was considered as one of the independent variables. Moreover, we were curious about whether EDModel could be generalized to hand-based pointing, although it was quite different from head-based pointing (discuss later). Besides, the study was designed to help us verify how μ_x of the distribution was affected by the movement amplitude, as an unsolved question from the first study.

4.1 Participants, Apparatus, and Materials

Another eighteen participants (4 females, 14 males) between the ages of 18-26 (mean = 21) were recruited from a local university campus. Data from the pre-experiment questionnaire suggested that thirteen of them had at least some prior VR experience. They all had a normal or corrected-to-normal vision. Among the participants, two of them were left-handed. We used the same devices and platform as the last experiment.

4.2 Experimental Task and Measurements

The task required the users to repeatedly point towards a fixed spherical target from the home button in a VR environment (see Figure 6A). For each trial, a participant needed to move the cursor to the highlighted target and click the trigger button to confirm the selection. After the trial ended (with a short sound), the participant would then move back to the home button and click the trigger to start the next trial. The participant must select the home button, which appeared to be much smaller than the target, correctly to proceed to the subsequent trial; this ensured they would start at the same position for each trial. This design is unlike the reciprocal-movement paradigm, in which an error might relate to errors that occurred on the previous trials [Schmidt et al. 1978]. While it posed more workload for participants (as they had to accurately select the home button and a back-and-forth movement only counted as one trial), it could possibly yield more accurate results. In addition, by controlling the movement amplitude A to be the same as the distance R between the center position of the head and the target position, this task design could help us find out how μ_x was affected by them after comparing with the results from Study 1. No feedback was provided to indicate the correctness of the selection.

We varied two independent variables in this experiment: movement amplitude R and target depth Z (see Figure 6A,B). R was described in the angular form, while Z was a distance value (recall the spherical coordinate system). All targets were set to a fixed radius r. From both r and Z, we would be able to calculate the visual width W_z of the target using the equation 3:

$$W_z = 2 \cdot \arcsin(\frac{r}{Z}) \quad (3)$$

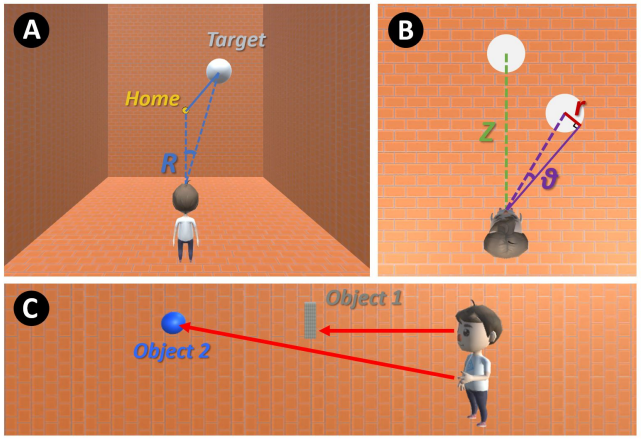

Fig. 6. (A) The angular form of movement amplitude R, and the home button and the target used in the second study. (B) The target with the same radius r located in different depths Z. (C) An illustration of the differences between head- and hand-based pointing.

The angular error distance of an endpoint $p = (x, y)$ was defined the same as the first study.

Apart from head-based pointing, we also introduced hand-based pointing in this study to test the generalizability of EDModel. The hand-based pointing technique, with which a visible ray was attached to and emitted from a hand-held controller, was different from the head-based pointing in three ways. First, the users would be able to see a green virtual ray emitted from the handheld controller when using hand-based pointing. Second, as shown in Figure 6C, users could select an occluded target through hand-based pointing, while the head-based pointing only allowed selection of visible targets [Argelaguet and Andujar 2013]. In this study, we placed the target to be very far from the viewpoint; hence the starting points for hand- and head-based pointing could be considered to be the same. By doing this, the selection differences caused by the two mechanisms could be mitigated. Third, the hand-based pointing was prone to the Heisenberg effect [Bowman et al. 2001], where the trigger confirmation could produce a change in the controller's orientation, thus leading to the wrong selection. This effect was not compensated in this study, as using the same controller for pointing and confirmation might be more natural in current VR systems.

In this study, static textures (walls in Figure 6A) were constructed to provide visual depth cues for targets located at different depths.

4.3 Design and Procedure

The study used a 6×3 within-subjects design with two factors: movement amplitude R (10° to 35°, with an increment step of 5°) and target depth Z (100m, 300m, and 500m, which corresponds to 5.73°, 1.91°, and 1.15° of visual width W_z). The level design of R allowed the targets to appear in a wider range than the first study, while still not requiring the participants to stretch their neck in an uncomfortable manner in the head pointing scenario. The level design of Z allowed two levels of visual widths to be within the range of the first study; but the third one ($Z = 100m$) had a much larger visual width because we aimed to test the reliability of EDModel for a much bigger (closer) target. The order of R was counterbalanced using a Latin Square design. For a given R, the three Z were presented randomly. For each $R \times Z$ combination, the target would appear in a random direction (10° to 350°, with an increment step of 20°; each direction appeared only once). The first two trials were discarded, leaving 20 timed repetitions. Two input mechanisms were used in this study: head-based pointing and hand-based pointing. The order of the two was also counterbalanced. In sum, we collected 6480 endpoints (6 $R \times 3$ $Z \times 18$ participants $\times$ 20 repetitions) for each of the two input mechanisms from the experiment.

The study lasted about 40-50 minutes for each participant. We employed a similar procedure to collect demographic information and introduce the task and VR devices. Participants then started the practice trials and calibrated their head positions. After, they proceeded to the formal trials. They were instructed to select the target as naturally as possible like in the first study. Participants were allowed to have a rest as long as they felt tired and were forced to have a break prior to switching the input mechanism. Most of them reported feeling slightly worn after the whole experiment.

4.4 Results

We used the same data pre-processing strategy as the first study. A total of 192 trials (2.96%) and 154 trials (2.38%) were removed from the head- and hand-based pointing data, respectively. The results from RM-ANOVA with Greenhouse-Geisser correction for both input mechanisms are summarized in Appendix C. We transferred Z to W_z using Equation 3 when conducting the linear regressions throughout the whole analysis.

4.4.1 Head-based Pointing. We ran a K-S test for normality and estimated μ, σ, and ρ as in the first study. Among the total of 324 sets (18 conditions $\times$ 18 participants), 1 set of endpoints in the x-axis was shown to be not normal. The μ_x, σ_x, and ρ of that set were replaced by averaging the other 17 sets of data in the same condition.

The RM-ANOVA indicated that R and Z had significant effects on μ_x, Z and $R \times Z$ had strong influences on σ_x, R and Z had main impacts on σ_y (see Appendix C for detailed statistics).

We applied the linear relationships found in the first study. The regression indicated strong linear relationship between W_z with σ_x ($R^2 = 0.99$) and W_z with σ_y ($R^2 = 0.99$), but not A with μ_x ($R^2 = 0.64$). As shown in Figure 7 (middle), when $R = 35$, the u_x appeared to have a much lower value than the others. If we only considered the first five datapoints, we would get a better fit with the linear regression ($R^2 = 0.88$). The linear relationships were $\sigma_x = 0.1140W_z + 0.4293$, $\mu_x = -0.0025R - 0.1919$ (omitting the last datapoint), and $\sigma_y = 0.0842W_z + 0.2800$.

Applying the regression with the new influential factors indicated by RM-ANOVA in this study, we found two new linear relationships using the averaged datapoints of each $R \times Z$ condition (totally 18 datapoints): $\mu_x = -0.0071R - 0.1203W_z + 0.2358$ ($\bar{R}^2 = 0.86$) and $\sigma_y = 0.0062R + 0.0842W_z + 0.1412$ ($\bar{R}^2 = 0.92$).

4.4.2 Hand-based Pointing. We ran a K-S test and estimated μ, σ, and ρ. Among the total of 324 sets, 1 set of endpoints in y-axis

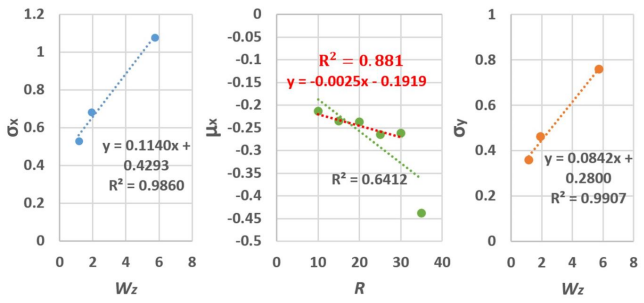

Fig. 7. Averaged σ_x of subjects' endpoint distributions for three levels of W_z (left), averaged μ_x for six levels of R (middle), and averaged σ_y for three levels of W_z (right).

was shown to be not normal. The μ_y, σ_y, and ρ of that set were replaced by the averaged value of the other 17 sets of data in the same condition.

The RM-ANOVA indicated that Z had significant effect on μ_x, R and Z both had strong influences on σ_x, R played an important role on μ_y, and R, Z, and $R \times Z$ had main impacts on σ_y.

Linear relationships found in the first study were applied. The regression indicated strong linear relationship between W_z with σ_x ($R^2 = 1.00$) and W_z with σ_y ($R^2 = 1.00$). The linear relationships were $\sigma_x = 0.1025W_z + 0.4146$ and $\sigma_y = 0.0679W_z + 0.3339$. There was no linear relationship found between R and μ_x.

Applying the regression with the new influential factors indicated by RM-ANOVAs, we found $\mu_x = -0.1441W_z + 0.2649$ ($R^2 = 1.00$) by fitting with 3 averaged datapoints which correspond to each W_z level, $\sigma_x = 0.0066R + 0.1025W_z + 0.2663$ ($\bar{R}^2 = 0.90$), and $\sigma_y = 0.0085R + 0.0679W_z + 0.1437$ ($\bar{R}^2 = 0.87$) by fitting 18 averaged datapoints. No linear relationship were found between R and μ_y.

4.5 Discussion

We first discuss the common features for both input mechanisms (head- and hand-based pointing). We then treat the two mechanisms separately and compare the results from this study to the previous one. After that, we answer the research questions we had before Study 2. Finally, we extend EDModel to more complex scenarios.

For both mechanisms, target depth Z can be transferred to visual width W_z. This could be because the relative size of the target was the dominant depth cue in our setting. Moreover, we found visual width W_z, like W, had strong linear relationships with both σ_x and σ_y. The coefficients of the linear equations varied a bit due to the different study settings and fewer number of tested levels, but were somewhat similar to the first study. This suggested that W_z played a similar role to target width W. Therefore, when adjusting the target depth in the design process, we could use Equation 3 to calculate the visual width W_z and then fit it as the target width parameter W into EDModel.

In contrast, as targets appeared at larger distances and in bigger sizes, some results were different from the previous study. As movement amplitude R increased, this factor started to influence σ_y in the distribution of both mechanisms. Larger movement amplitude R caused the endpoints of the y-axis to become more sparse. However, visual size W_z led to much large influence on σ_y than R, as suggested by a separate linear regression test that included both factors. It could be essential to consider the effect of R on σ_y when the movement amplitude is relatively large. In addition, fitting 18 datapoints ($6R \times 3Z$) to σ_y with both factors offered better results ($\bar{R}^2 = 0.92$ for head and $\bar{R}^2 = 0.87$ for hand) than fitting the same 18 datapoints with W_z alone ($R^2 = 0.85$ for head and $R^2 = 0.69$ for hand).

For head-based pointing mechanism, as shown in Figure 7, $R = 35°$ caused a significant drop of μ_x. In this case, we inferred that the neck muscle constrained the pointing severely and caused a salient "lazy effect" found in the first study. Furthermore, as the targets became much larger ($W_z = 5.73°$ in the extreme case), the factor W_z started to influence μ_x. This evidence supported the inference made by previous researchers (e.g., [Grossman and Balakrishnan 2005]) in that as target sizes grow, the center of the distribution could be placed closer to the side of the target. The linear regression combined both factors (R and W_z) was shown to provide a better fit ($\bar{R}^2 = 0.86$) than single factor based regression. Hence, when the movement amplitude R and target size W_z were large (or target appeared to be very close), we should apply linear regression with both factors to adjust EDModel.

Hand-based pointing acted differently, as the constraint imposed by muscle had a much smaller effect (R did not influence μ_x in a significant way), leaving W_z to be the only factor affecting μ_x. Movement amplitude R also had an impact on σ_x which supported the finding from Grossman and Balakrishnan [Grossman and Balakrishnan 2005]—the spread of hit in x-axis increased when the movement amplitude increased. However, the effect of R on σ_x was much smaller than W_z. A linear regression combining both R and W_z was shown to have a better fit ($\bar{R}^2 = 0.90$) for σ_x.

Similar to the previous study, the correlation coefficient ρ between X and Y was extremely small for both head- and hand-based pointing ($\rho = -0.006$ and $\rho = 0.031$, respectively), thus we could set $\rho = 0$. Besides, μ_y was also approximate to zero for both mechanisms ($\mu_y = -0.012$ for head and $\mu_y = -0.041$ for hand).

In response to the question raised at the beginning of Study 2 about how μ_x was actually affected by the movement amplitude in head-based pointing: after comparing the μ_x values in the similar range from both studies ($W \in [1, 2]$ and $R \in [15, 20]$), our current answer is that μ_x will decrease when the distance between the target position and the center position of the head increases. That is, the muscle will constrain the movement—the more stretched the muscle, the lazier the user will become. It probably does not relate to the starting position of the head. However, as we did not vary the starting positions, and we examined multiple factors in this study which could potentially mitigate the effect of the movement amplitude, we may need further research to verify this claim.

In sum, for targets appearing at wider ranges and in larger sizes, the previous simpler EDModel might not be enough. A more complex EDModel with additional fitting parameters is needed. Besides, it could be more appropriate to replace movement amplitude A in Study 1 with R which is the angular distance between the target position and the center position of the head. According to Study

2, EDModel can be extended with the following parameters for head-based pointing:

$$\boldsymbol{\mu} = \begin{bmatrix} lR + mW + n \\ 0 \end{bmatrix}, \Sigma = \begin{bmatrix} (gW + h)^2 & 0 \\ 0 & (iR + jW + k)^2 \end{bmatrix} \quad (4)$$

where our data suggest that $g = 0.1140$, $h = 0.4293$, $i = 0.0062$, $j = 0.0842$, $k = 0.1412$, $l = -0.0071$, $m = -0.1203$, and $n = 0.2358$. For hand-based pointing, due to its differences from head-based pointing, we use a separate list of parameters:

$$\boldsymbol{\mu} = \begin{bmatrix} uW + v \\ 0 \end{bmatrix}, \Sigma = \begin{bmatrix} (oR + pW + q)^2 & 0 \\ 0 & (rR + sW + t)^2 \end{bmatrix} \quad (5)$$

where our data indicate that $o = 0.0066$, $p = 0.1025$, $q = 0.2663$, $r = 0.0085$, $s = 0.0679$, $t = 0.1437$, $u = -0.1441$, and $v = 0.2649$.

When targets with a size $W < 4.5°$ appeared with $R < 30°$, a simple EDModel as in the first study could produce satisfying results. However, when the target appeared in a broader range with a larger size, the complex EDModel is needed.

5 SUMMARY OF FINDINGS

We briefly summarize the main findings from both studies below.

Based on the data from the first experiment, we can see that the endpoint distribution of pointing selection in VEs is bivariate-Gaussian. The values of σ_x and σ_y are linearly correlated with target width W, while μ_y has a linear relationship with movement amplitude A (or R, which is the distance between the target position and the center position of the head). No correlation ρ between X and Y was found, and there were no other main effects either. Our initial EDModel is represented as Equation 2 (replacing A with $2R$ according to our finding in the second study).

After testing EDModel in more complex scenarios, we found that target depth Z could be transferred to target width W for model fitting. In addition, we found that as targets appeared in wider visual angles and had larger sizes, more factors would start to have impacts on different the parameters of the endpoint distribution. Due to their unique features, EDModel is extended for head- and hand-based pointing separately for complex conditions (see Equation 4 and 5). We have also found that muscle constraints might induce a "lazy" effect with head-based pointing.

6 APPLICATIONS

In this section, we demonstrate the usefulness of EDModel in three different applications that are related to pointing selection tasks in VR: (1) correcting the bias in Fitts's law, (2) predicting selection accuracy, and (3) using a selection technique based on Bayes' theorem. Because of space limitations, the derivatives are all based on the simpler EDModel (but the more complex model could be easily used instead).

6.1 Correcting the Bias in Fitts's Law

Fitts's law [Fitts 1954], usually formulated as Equation 6 [Soukoreff and MacKenzie 2004], has been widely used in HCI to predict the movement time MT to acquire a target with size W and at a distance A. In the equation, a_F and b_F are regressions coefficients, while the log term is named as the index of difficulty (ID) [2].

$$MT = a_F + b_F \log_2(\frac{A}{W} + 1) \quad (6)$$

Fitts's law assumes a 4% error rate according to its information theory basis [MacKenzie 1992; Soukoreff and MacKenzie 2004]. However, users often apply different speed-accuracy strategies according to the properties of the target which might lead to a deviation of the observed error rates from 4%. In this condition, Fitt's law might produce a biased result. When this happens, a post-hoc correction can be applied using the effective (observed) target width W_e and movement amplitude A_e to replace the nominal width W and amplitude A (see Equation 7) [Crossman 1957; Welford 1968; Wobbrock et al. 2011b]. The W_e is usually determined using Equation 8 by fitting the observed endpoint data. The A_e is the real movement distance from the starting point to the effective target center. Although the adjustment was shown to be not always entirely corrective [Zhai et al. 2004] or questionable [Gori et al. 2017], it is still useful in many cases [Soukoreff and MacKenzie 2004].

$$ID_e = \log_2(\frac{A_e}{W_e} + 1) \quad (7)$$

$$W_e = \sqrt{2\pi e}\sigma = 4.133\sigma \quad (8)$$

6.1.1 Calculating ID_e with EDModel. With EDModel, collecting the endpoint data of each new $A \times W$ combination for the adjustment is not needed. Our model can aid the calculation of the effective A_e and W_e either univariately (A_x and W_x) or bivariately ($A_{x,y}$ and $W_{x,y}$) [Wobbrock et al. 2011b] for unseen targets with arbitrary A and W properties. For uni-correction, we use Equation 9 and 10 to replace the corresponding μ and σ in A_e and W_e, and derive the corrected Fitts's law as Equation 11.

$$\mu_x = eA + f \quad (9)$$

$$\sigma_x = aW + b \quad (10)$$

$$MT = a_F + b_F \log_2(\frac{A + eA + f}{\sqrt{2\pi e}(aW + b)} + 1) \quad (11)$$

For bi-correction, the μ and σ are substituted using Equation 12 and 13. We adjusted Fitts's law as Equation 14.

$$\mu_{x,y} = \mu_x + \mu_y = eA + f \quad (12)$$

$$\sigma_{x,y} = \sqrt{\sigma_x^2 + \sigma_y^2} = \sqrt{(aW + b)^2 + (cW + d)^2} \quad (13)$$

$$MT = a_F + b_F \log_2(\frac{A + eA + f}{\sqrt{2\pi e[(aW + b)^2 + (cW + d)^2]}} + 1) \quad (14)$$

6.1.2 Model Evaluation. We tested the correction made by EDModel using the head-based pointing data collected from Study 1 and Study 2. As shown in Table 2, the correction results produced by EDModel are very similar to the correction results based on empirical data, while the corrected and uncorrected coefficients seem to have large disparities. We also noticed that for the data from Study 1, the correction seems to lower the fitting correlation R^2. As noted by Fitts himself and other researchers [Fitts and Radford 1966; Soukoreff and MacKenzie 2004; Wobbrock et al. 2011b], it is typical

[2] We use a_F and b_F for the coefficients of Fitts's law here to distinguish with the a and b in EDModel.

Table 2. Results of Fitts's law regression coefficients (a_F and b_F) and R^2 in Study 1 and Study 2 using no correction, direct uni- and bi-correction based on the empirical data, and EDModel-based uni- and bi-correction.

Model	Study 1			Study 2		
	a_F	b_F	R^2	a_F	b_F	R^2
No Corr.	0.25	0.23	0.96	0.41	0.19	0.92
Direct Uni-Corr.	-0.35	0.40	0.87	0.10	0.32	0.98
Direct Bi-Corr.	-0.28	0.42	0.89	0.13	0.34	0.98
EDModel Uni-Corr.	-0.38	0.40	0.89	0.15	0.30	0.95
EDModel Bi-Corr.	-0.29	0.42	0.89	0.15	0.33	0.96

and appropriate for models using corrected ID_e instead of nominal ID, even if the correlations are lower.

Overall, EDModel could produce promising correction results (close to the results fitted with empirical data) for Fitts's law when extending to unseen $W \times A$ combinations.

6.2 Predicting Selection Accuracy

Estimating selection accuracy is important for the design of graphical user interfaces and games. Following Wobbrock et al. [2008, 2011a], researchers have more recently explored modeling selection accuracy in various domains, including finger touch selection [Bi and Zhai 2016] and moving target selection [Huang and Lee 2019; Huang et al. 2018; Lee et al. 2018; Lee and Oulasvirta 2016; Lee et al. 2019; Park et al. 2018]. Here we demonstrate how Bi's approach [Bi and Zhai 2016] can be combined with EDModel to assist in the estimation of pointing selection accuracy in VR.

6.2.1 Combining EDModel with Bi's Method. The probability of successfully acquiring a target is the probability of the selection endpoint falling within the target boundaries [Bi and Zhai 2016]. As such, the success rate of acquiring the target D can be calculated through the probability density function (pdf, see Equation 20 in Appendix B) of the endpoint distribution using

$$y = \iint_D f(\begin{bmatrix} x \\ y \end{bmatrix}, \boldsymbol{\mu}, \Sigma)\, dxdy \tag{15}$$

According to the results from both studies, $\rho = 0$ and $\mu_y = 0$, such that Equation 15 can be expanded and simplified to:

$$y = \iint_D \frac{1}{2\pi\sigma_x\sigma_y} \exp\left(-\frac{(x-\mu_x)^2}{2\sigma_x^2} - \frac{y^2}{2\sigma_y^2}\right) dxdy \tag{16}$$

Replacing μ_x, σ_x, and σ_y with the parameters found from Study 1 and Study 2, we are able to estimate the selection accuracy.

6.2.2 Model Evaluation. We evaluated the results of the EDModel-based accuracy prediction using the head-based pointing data from Study 1 and Study 2. We used Wobbrock's error model [Wobbrock et al. 2011a] as a baseline (see Appendix D for a simple explanation of the model). According to Wobbrock et al. [2008], the a and b parameters of the baseline model were adjusted with the bivariate post-hoc correction [Crossman 1957; Wobbrock et al. 2011b]. The prediction results are presented in Figure 8.

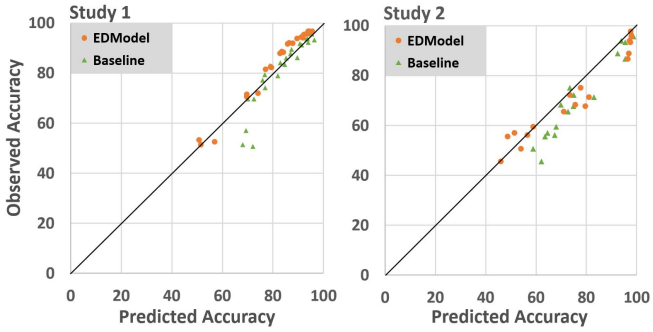

Fig. 8. Accuracy prediction results for head-based pointing selection from Study 1 and Study 2. EDModel-based prediction led to a slightly better fit than the baseline model.

The EDModel-based prediction fit the observed accuracy well ($R^2 = 0.95$, Mean Absolute Error (MAE) = 3.14% for Study 1; $R^2 = 0.91$, MAE = 4.58% for Study 2) and achieved a slightly better performance than the baseline model ($R^2 = 0.88$, MAE = 3.56% for Study 1; $R^2 = 0.91$, MAE = 6.10% for Study 2).

In sum, EDModel-based accuracy prediction could be a reliable method for predicting selection accuracy in VR and hence can be useful to UI designers to support their decisions.

6.3 BayesPointer for Pointing Selection in VR

Recent work [Huang and Lee 2019; Huang et al. 2018; Li et al. 2018] has proposed an efficient selection technique based on pointing distribution called BayesPointer for moving targets in 1D and 2D space. The basic idea of this technique is to automatically choose the target with the maximum posterior probability in Bayes' theorem [Bi and Zhai 2013]. Similar approaches have also been applied in text entry to infer a user's intended text from a noisy input [Goodman et al. 2002; Yu et al. 2017].

6.3.1 Combining BayesPointer with EDModel. With our endpoint distribution model, BayesPointer can be transferred for pointing tasks in VR. Assuming the list of targets $T = \{t_1, t_2, ..., t_n\}$, the probability of selecting a target t with an endpoint s is $P(t|s)$. According to Bayes' theorem (Equation 17), $P(t|s)$ can be calculated via (1) prior probability $P(t)$ which is usually set to $1/n$; (2) input occurring probability $P(s)$ which is a constant value; and (3) the likelihood function $P(s|t)$ which can be computed from the probability density function (pdf, see Equation 20 in Appendix B) of EDModel.

$$P(t|s) = \frac{P(s|t)P(t)}{P(s)} \tag{17}$$

Because $P(t)$ and $P(s)$ are the same for each potential target, the intended target t^* can be chosen using Equation 18–this is the decision-making strategy of BayesPointer. Similar to [Li et al. 2018], the auto-selection mechanism is only triggered when the pointer falls into the range within the $3W$ contour line of the target.

$$t^* = \arg\max_t P(s|t) = \arg\max_t f(s, \boldsymbol{\mu}, \Sigma) \tag{18}$$

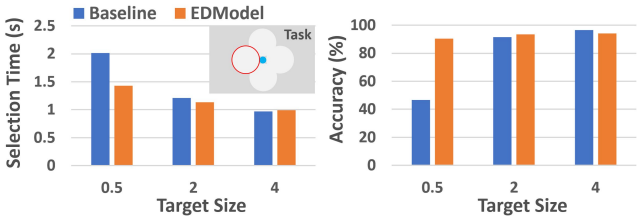

Fig. 9. Selection task and study results when comparing raycasting and EDModel-based BayesPointer. The later technique performed much better in selecting small targets regarding both selection time and accuracy.

6.3.2 Technique Evaluation. We conducted a small study with 4 participants to demonstrate the usefulness of BayesPointer with our endpoint distribution model for pointing selection tasks in VR.

The task design was similar to our first study, with four distractors surrounding the goal target (see Figure 9). The target width W had three levels (0.5°, 2°, and 4°), while the width of the distractors remained the same (2°). For each condition, we ran two rounds of the Fitts's ring ($R = 20°$). To assist this pointing task, EDModel-based BayesPointer would highlight the intended target with a red border. Raycasting was used as the baseline technique, and the target would be highlighted only if the user was pointing on it. In total, we collected $3W \times 2$ techniques $\times$ 4 participants $\times$ 20 repetitions = 480 trials of data.

As shown in Figure 9, EDModel-based BayesPointer achieved much better performance in terms of both shorter selection time and higher accuracy than the baseline technique in selecting small targets. Both techniques had similar performance for selecting medium and large size target. We envisioned EDModel-based BayesPointer could be particularly helpful for selection small and/or far-away targets. While evaluating this selection technique was not our primary focus, we used this small study to show that the difference between the EDModel-based technique and the baseline one was significant enough. Because of space limitations, we leave larger studies with more complex experiment settings for future work.

7 LIMITATIONS AND FUTURE WORK

In this section, we describe some limitations of the current work and possible avenues for future research. First, although we tried to position the targets in wide visual areas in our studies, the angles between the targets and users' view were still within the FoV of the head-mounted displays (HMDs) device (a bit larger in some conditions). In addition, although we considered targets with a visual width at around 6° which appeared to be large, their sizes could be further enlarged. Future work could explore targets located far from the user's center viewing angle and outside of their view (i.e., off-screen targets [Yu et al. 2019]). Having these additional conditions into one single model could further extend its usefulness and make it more general. Second, as suggested by previous research, a target's placement direction could also have an impact on its selection [Hancock and Booth 2004]. This aspect was outside of the scope of this work and was not explored. Future work could try to integrate the direction parameter into the model. Moreover, future research could examine targets with arbitrary shapes [Grossman et al. 2007], other input devices or methods, and displays which have different features from VR HMDs, like screen displays coupled with stereo glasses [Barrera Machuca and Stuerzlinger 2019]. Additionally, the stereo acuity of participants could have an impact on task performance with targets of different depths and may probably be useful to consider in future research.

We also look forward to future research that could help develop other modeling possibilities for endpoint distribution in VR using our open-sourced dataset or conducting user studies with other parameters and scenarios. Finally, there are other applications that can leverage our endpoint distribution model to make the interaction more efficient and usable. We hope to see more of such applications in the future.

8 CONCLUSION

In this paper, we present EDModel, an endpoint distribution model which is based on the bivariate-Gaussian distribution for pointing selection in virtual reality environments. Through two user studies, we show how different factors, such as target width, movement amplitude and target depth, could affect the endpoint distribution. Two versions of EDModel are proposed, one dealing with simpler scenarios and the other more complex conditions. The simpler model uses fewer parameters, which are relaxed in the complex EDModel to deal with targets that are larger and have broader ranges. We also describe three current applications that can use EDModel. The results of their evaluation show that EDModel can achieve high prediction accuracy for selection endpoints and could be suitable for various applications in virtual reality systems.

ACKNOWLEDGMENTS

We want to thank our participants for their time and the reviewers for the comments and suggestions that helped improve our paper. We also would like to thank Nan Zhu from Xi'an Jiaotong-Liverpool University for coordinating the recruitment of some participants. This research was supported by AI University Research Centre (AI-URC) at Xi'an Jiaotong-Liverpool University (XJTLU), XJTLU Key Program Special Fund (KSF-A-03 and KSF-02), and XJTLU Research Development Fund.

REFERENCES

Ferran Argelaguet and Carlos Andujar. 2009. Efficient 3D Pointing Selection in Cluttered Virtual Environments. *IEEE Computer Graphics and Applications* 29, 6 (Nov 2009), 34–43. https://doi.org/10.1109/MCG.2009.117

Ferran Argelaguet and Carlos Andujar. 2013. A survey of 3D object selection techniques for virtual environments. *Computers & Graphics* 37, 3 (2013), 121–136.

Marc Baloup, Thomas Pietrzak, and Géry Casiez. 2019. RayCursor: A 3D Pointing Facilitation Technique Based on Raycasting. In *Proceedings of the 2019 CHI Conference on Human Factors in Computing Systems (CHI '19)*. ACM, New York, NY, USA, Article 101, 12 pages. https://doi.org/10.1145/3290605.3300331

Nikola Banovic, Tovi Grossman, and George Fitzmaurice. 2013. The Effect of Time-based Cost of Error in Target-directed Pointing Tasks. In *Proceedings of the SIGCHI Conference on Human Factors in Computing Systems (CHI '13)*. ACM, New York, NY, USA, 1373–1382. https://doi.org/10.1145/2470654.2466181

Mayra Donaji Barrera Machuca and Wolfgang Stuerzlinger. 2019. The Effect of Stereo Display Deficiencies on Virtual Hand Pointing. In *Proceedings of the 2019 CHI Conference on Human Factors in Computing Systems (CHI '19)*. ACM, New York, NY, USA, Article 207, 14 pages. https://doi.org/10.1145/3290605.3300437

Dimitri P. Bertsekas and John N. Tsitsiklis. 2002. *Introduction to probability*. Vol. 1. Athena Scientific Belmont, MA.

Xiaojun Bi, Yang Li, and Shumin Zhai. 2013. FFitts Law: Modeling Finger Touch with Fitts' Law. In *Proceedings of the SIGCHI Conference on Human Factors in Computing*

Systems (CHI '13). ACM, New York, NY, USA, 1363–1372. https://doi.org/10.1145/2470654.2466180

Xiaojun Bi and Shumin Zhai. 2013. Bayesian Touch: A Statistical Criterion of Target Selection with Finger Touch. In *Proceedings of the 26th Annual ACM Symposium on User Interface Software and Technology (UIST '13)*. ACM, New York, NY, USA, 51–60. https://doi.org/10.1145/2501988.2502058

Xiaojun Bi and Shumin Zhai. 2016. Predicting Finger-Touch Accuracy Based on the Dual Gaussian Distribution Model. In *Proceedings of the 29th Annual Symposium on User Interface Software and Technology (UIST '16)*. ACM, New York, NY, USA, 313–319. https://doi.org/10.1145/2984511.2984546

Doug Bowman, Ernst Kruijff, Joseph J LaViola Jr, and Ivan P Poupyrev. 2004. *3D User interfaces: theory and practice, CourseSmart eTextbook*. Addison-Wesley.

Doug Bowman, Chadwick Wingrave, Joshua Campbell, and Vinh Ly. 2001. Using pinch gloves (tm) for both natural and abstract interaction techniques in virtual environments. (2001).

ERFW Crossman. 1957. The speed and accuracy of simple hand movements. *The nature and acquisition of industrial skills* (1957).

Paul M. Fitts. 1954. The information capacity of the human motor system in controlling the amplitude of movement. *Journal of experimental psychology* 47, 6 (1954), 381.

Paul M. Fitts and Barbara K. Radford. 1966. Information capacity of discrete motor responses under different cognitive sets. *Journal of Experimental Psychology* 71, 4 (1966), 475.

Joshua Goodman, Gina Venolia, Keith Steury, and Chauncey Parker. 2002. Language Modeling for Soft Keyboards. In *Proceedings of the 7th International Conference on Intelligent User Interfaces (IUI '02)*. ACM, New York, NY, USA, 194–195. https://doi.org/10.1145/502716.502753

Julien Gori, Olivier Rioul, and Yves Guiard. 2017. To Miss is Human: Information-Theoretic Rationale for Target Misses in Fitts' Law. In *Proceedings of the 2017 CHI Conference on Human Factors in Computing Systems (CHI '17)*. ACM, New York, NY, USA, 260–264. https://doi.org/10.1145/3025453.3025660

Tovi Grossman and Ravin Balakrishnan. 2005. A Probabilistic Approach to Modeling Two-dimensional Pointing. *ACM Trans. Comput.-Hum. Interact.* 12, 3 (Sept. 2005), 435–459. https://doi.org/10.1145/1096737.1096741

Tovi Grossman, Nicholas Kong, and Ravin Balakrishnan. 2007. Modeling Pointing at Targets of Arbitrary Shapes. In *Proceedings of the SIGCHI Conference on Human Factors in Computing Systems (CHI '07)*. ACM, New York, NY, USA, 463–472. https://doi.org/10.1145/1240624.1240700

Yves Guiard, Halla B. Olafsdottir, and Simon T. Perrault. 2011. Fitt's Law As an Explicit Time/Error Trade-off. In *Proceedings of the SIGCHI Conference on Human Factors in Computing Systems (CHI '11)*. ACM, New York, NY, USA, 1619–1628. https://doi.org/10.1145/1978942.1979179

Yves Guiard and Olivier Rioul. 2015. A Mathematical Description of the Speed/Accuracy Trade-off of Aimed Movement. In *Proceedings of the 2015 British HCI Conference (British HCI '15)*. ACM, New York, NY, USA, 91–100. https://doi.org/10.1145/2783446.2783574

Mark S. Hancock and Kellogg S. Booth. 2004. Improving Menu Placement Strategies for Pen Input. In *Proceedings of Graphics Interface 2004 (GI '04)*. Canadian Human-Computer Communications Society, School of Computer Science, University of Waterloo, Waterloo, Ontario, Canada, 221–230. http://dl.acm.org/citation.cfm?id=1006058.1006085

Jin Huang and Byungjoo Lee. 2019. Modeling Error Rates in Spatiotemporal Moving Target Selection. In *Extended Abstracts of the 2019 CHI Conference on Human Factors in Computing Systems (CHI EA '19)*. ACM, New York, NY, USA, Article LBW2411, 6 pages. https://doi.org/10.1145/3290607.3313077

Jin Huang, Feng Tian, Xiangmin Fan, Xiaolong (Luke) Zhang, and Shumin Zhai. 2018. Understanding the Uncertainty in 1D Unidirectional Moving Target Selection. In *Proceedings of the 2018 CHI Conference on Human Factors in Computing Systems (CHI '18)*. ACM, New York, NY, USA, Article 237, 12 pages. https://doi.org/10.1145/3173574.3173811

ISO. 2000. ISO 9241-9:2000. *Ergonomic requirements for office work with visual display terminals (VDTs) - Part 9 - Requirements for non-keyboard input devices* (2000).

ISO. 2009. ISO80000-2: 2009. *Quantities and units–Part 2: Mathematical signs and symbols to be used in the natural sciences and technology* (2009).

Regis Kopper, Doug A. Bowman, Mara G. Silva, and Ryan P. McMahan. 2010. A human motor behavior model for distal pointing tasks. *International Journal of Human-Computer Studies* 68, 10 (2010), 603 – 615. https://doi.org/10.1016/j.ijhcs.2010.05.001

Samuel Kotz, Narayanaswamy Balakrishnan, and Norman L. Johnson. 2004. *Continuous multivariate distributions, Volume 1: Models and applications*. Vol. 1. John Wiley & Sons.

Byungjoo Lee, Sunjun Kim, Antti Oulasvirta, Jong-In Lee, and Eunji Park. 2018. Moving Target Selection: A Cue Integration Model. In *Proceedings of the 2018 CHI Conference on Human Factors in Computing Systems (CHI '18)*. ACM, New York, NY, USA, Article 230, 12 pages. https://doi.org/10.1145/3173574.3173804

Byungjoo Lee and Antti Oulasvirta. 2016. Modelling Error Rates in Temporal Pointing. In *Proceedings of the 2016 CHI Conference on Human Factors in Computing Systems (CHI '16)*. ACM, New York, NY, USA, 1857–1868. https://doi.org/10.1145/2858036.2858143

Injung Lee, Sunjun Kim, and Byungjoo Lee. 2019. Geometrically Compensating Effect of End-to-End Latency in Moving-Target Selection Games. In *Proceedings of the 2019 CHI Conference on Human Factors in Computing Systems (CHI '19)*. ACM, New York, NY, USA, 560:1–560:12. https://doi.org/10.1145/3290605.3300790

Nianlong Li, Feng Tian, Jin Huang, Xiangmin Fan, and Hongan Wang. 2018. 2D-BayesPointer: An Implicit Moving Target Selection Technique Enabled by Human Performance Modeling. In *Extended Abstracts of the 2018 CHI Conference on Human Factors in Computing Systems (CHI EA '18)*. ACM, New York, NY, USA, Article LBW125, 6 pages. https://doi.org/10.1145/3170427.3188520

I. Scott MacKenzie. 1992. Fitts' law as a research and design tool in human-computer interaction. *Human-computer interaction* 7, 1 (1992), 91–139.

I. Scott MacKenzie and Poika Isokoski. 2008. Fitts' Throughput and the Speed-accuracy Tradeoff. In *Proceedings of the SIGCHI Conference on Human Factors in Computing Systems (CHI '08)*. ACM, New York, NY, USA, 1633–1636. https://doi.org/10.1145/1357054.1357308

Atsuo Murata. 1999. Extending Effective Target Width in Fitts' Law to a Two-Dimensional Pointing Task. *International Journal of Human-Computer Interaction* 11, 2 (1999), 137–152. https://doi.org/10.1207/S153275901102_4

Eunji Park, Hyunju Kim, Injung Lee, and Byungjoo Lee. 2018. Whether Moving or Not: Modeling and Predicting Error Rates in Pointing Regardless of Target Motion. *arXiv preprint arXiv:1806.02973* (2018).

Julian Petford, Miguel A. Nacenta, and Carl Gutwin. 2018. Pointing All Around You: Selection Performance of Mouse and Ray-Cast Pointing in Full-Coverage Displays. In *Proceedings of the 2018 CHI Conference on Human Factors in Computing Systems (CHI '18)*. ACM, New York, NY, USA, Article 533, 14 pages. https://doi.org/10.1145/3173574.3174107

Réjean Plamondon and Adel M Alimi. 1997. Speed/accuracy trade-offs in target-directed movements. *Behavioral and brain sciences* 20, 2 (1997), 279–303.

Yuan Yuan Qian and Robert J. Teather. 2017. The Eyes Don't Have It: An Empirical Comparison of Head-based and Eye-based Selection in Virtual Reality. In *Proceedings of the 5th Symposium on Spatial User Interaction (SUI '17)*. ACM, New York, NY, USA, 91–98. https://doi.org/10.1145/3131277.3132182

Richard A. Schmidt, Howard Zelaznik, Brian Hawkins, James S. Frank, and John T. Quinn Jr. 1979. Motor-output variability: a theory for the accuracy of rapid motor acts. *Psychological review* 86, 5 (1979), 415.

Richard A. Schmidt, Howard N. Zelaznik, and James S. Frank. 1978. 9 - Sources of Inaccuracy in Rapid Movement. In *Information Processing in Motor Control and Learning*, George E. Stelmach (Ed.). Academic Press, 183 – 203. https://doi.org/10.1016/B978-0-12-665960-3.50014-1

R. William Soukoreff and I. Scott MacKenzie. 2004. Towards a standard for pointing device evaluation, perspectives on 27 years of Fitts' law research in HCI. *International journal of human-computer studies* 61, 6 (2004), 751–789.

R. William Soukoreff and I. Scott MacKenzie. 2009. An informatic rationale for the speed-accuracy trade-off. In *2009 IEEE International Conference on Systems, Man and Cybernetics*. 2890–2896. https://doi.org/10.1109/ICSMC.2009.5346580

Huawei Tu, Susu Huang, Jiabin Yuan, Xiangshi Ren, and Feng Tian. 2019. Crossing-Based Selection with Virtual Reality Head-Mounted Displays. In *Proceedings of the 2019 CHI Conference on Human Factors in Computing Systems (CHI '19)*. ACM, New York, NY, USA, Article 618, 14 pages. https://doi.org/10.1145/3290605.3300848

Lode Vanacken, Tovi Grossman, and Karin Coninx. 2007. Exploring the Effects of Environment Density and Target Visibility on Object Selection in 3D Virtual Environments. In *2007 IEEE Symposium on 3D User Interfaces*. https://doi.org/10.1109/3DUI.2007.340783

Feng Wang and Xiangshi Ren. 2009. Empirical Evaluation for Finger Input Properties in Multi-touch Interaction. In *Proceedings of the SIGCHI Conference on Human Factors in Computing Systems (CHI '09)*. ACM, New York, NY, USA, 1063–1072. https://doi.org/10.1145/1518701.1518864

Alan Traviss Welford. 1968. Fundamentals of skill. (1968).

Chadwick A. Wingrave and Doug A. Bowman. 2005. Baseline Factors for Raycasting Selection. In *Proceedings of Virtual Reality International*.

Jacob O. Wobbrock, Edward Cutrell, Susumu Harada, and I. Scott MacKenzie. 2008. An Error Model for Pointing Based on Fitts' Law. In *Proceedings of the SIGCHI Conference on Human Factors in Computing Systems (CHI '08)*. ACM, New York, NY, USA, 1613–1622. https://doi.org/10.1145/1357054.1357306

Jacob O. Wobbrock, Alex Jansen, and Kristen Shinohara. 2011a. Modeling and Predicting Pointing Errors in Two Dimensions. In *Proceedings of the SIGCHI Conference on Human Factors in Computing Systems (CHI '11)*. ACM, New York, NY, USA, 1653–1656. https://doi.org/10.1145/1978942.1979183

Jacob O. Wobbrock, Kristen Shinohara, and Alex Jansen. 2011b. The effects of task dimensionality, endpoint deviation, throughput calculation, and experiment design on pointing measures and models. In *Proceedings of the SIGCHI Conference on Human Factors in Computing Systems*. ACM, 1639–1648.

Shota Yamanaka. 2018a. Effect of Gaps with Penal Distractors Imposing Time Penalty in Touch-pointing Tasks. In *Proceedings of the 20th International Conference on Human-Computer Interaction with Mobile Devices and Services (MobileHCI '18)*. ACM, New York, NY, USA, Article 21, 11 pages. https://doi.org/10.1145/3229434.3229435

Shota Yamanaka. 2018b. Risk Effects of Surrounding Distractors Imposing Time Penalty in Touch-Pointing Tasks. In *Proceedings of the 2018 ACM International Conference on Interactive Surfaces and Spaces (ISS '18)*. ACM, New York, NY, USA, 129–135. https://doi.org/10.1145/3279778.3279781

Chun Yu, Yizheng Gu, Zhican Yang, Xin Yi, Hengliang Luo, and Yuanchun Shi. 2017. Tap, Dwell or Gesture?: Exploring Head-Based Text Entry Techniques for HMDs. In *Proceedings of the 2017 CHI Conference on Human Factors in Computing Systems (CHI '17)*. ACM, New York, NY, USA, 4479–4488. https://doi.org/10.1145/3025453.3025964

Difeng Yu, Hai-Ning Liang, Kaixuan Fan, Heng Zhang, Charles Fleming, and Konstantinos Papangelis. 2019. Design and Evaluation of Visualization Techniques of Off-Screen and Occluded Targets in Virtual Reality Environments. *IEEE Transactions on Visualization and Computer Graphics* (2019). https://doi.org/10.1109/TVCG.2019.2905580

Shumin Zhai, Jing Kong, and Xiangshi Ren. 2004. Speed-accuracy tradeoff in Fitts' law tasks-on the equivalency of actual and nominal pointing precision. *International Journal of Human-Computer Studies* 61, 6 (2004), 823 – 856. https://doi.org/10.1016/j.ijhcs.2004.09.007

A OPEN-SOURCED DATASET

The dataset we have collected in Study 1 and Study 2 is open-sourced, available at https://github.com/Davin-Yu/Endpoints-Modeling. The dataset contains 20640 pointing selection trials (including task settings, endpoint locations, and task completion time) collected in the VR environments. We also include the data processing scripts for replication and future exploration purpose. While most of the previous work did not make their dataset public available, we hope this dataset could provide an early testbed for future new models.

B BIVARIATE-GAUSSIAN DISTRIBUTION

The bivariate-Gaussian distribution (or bivariate-normal distribution) extends the univariate-Gaussian distribution to two dimensions. It is a distribution of two variables $\boldsymbol{X}$ and $\boldsymbol{Y}$, where each single variable has a Gaussian distribution (for formal mathematical definitions, please refer to [Bertsekas and Tsitsiklis 2002; Kotz et al. 2004]). If $\boldsymbol{X}$ and $\boldsymbol{Y}$ are both normally distributed and independent, then it implies the pair $(\boldsymbol{X}, \boldsymbol{Y})$ must have bivariate-Gaussian distribution.

A bivariate-Gaussian distribution contains: a mean vector $\boldsymbol{\mu}$ and the covariance matrix Σ, where

$$\boldsymbol{\mu} = \begin{bmatrix} \mu_x \\ \mu_y \end{bmatrix}, \Sigma = \begin{bmatrix} \sigma_x^2 & \rho\sigma_x\sigma_y \\ \rho\sigma_x\sigma_y & \sigma_y^2 \end{bmatrix} \tag{19}$$

in which μ_x and μ_y are the mean, σ_x and σ_y are the standard deviation of the distribution of the variable $\boldsymbol{X}$ and $\boldsymbol{Y}$, and ρ is the correlation between $\boldsymbol{X}$ and $\boldsymbol{Y}$. The probability density function (pdf) for bivariate-Gaussian distribution can be calculated as

$$y = f(\boldsymbol{x}, \boldsymbol{\mu}, \Sigma) = \frac{1}{2\pi\sqrt{|\Sigma|}} \exp(-\frac{1}{2}(\boldsymbol{x} - \boldsymbol{\mu})\Sigma^{-1}(\boldsymbol{x} - \boldsymbol{\mu})') \tag{20}$$

where $\boldsymbol{x}$ is a real 2-dimensional column vector and $|\Sigma|$ is the determinant of Σ ($|\Sigma| \equiv \det\Sigma$).

C RM-ANOVA RESULTS IN STUDY 2

The results of RM-ANOVAs in Study 2. Only the factors which had significant main effects on DV were reported.

Factor	*DV*	df_{effect}	df_{error}	F	p	η_p^2	Input
R	μ_x	3.505	59.579	4.154	.007	.196	Head
Z	μ_x	1.057	17.964	29.721	.000	.636	Head
Z	σ_x	1.214	20.646	118.114	.000	.874	Head
$R \times Z$	σ_x	5.776	98.192	2.308	.042	.120	Head
R	σ_y	3.438	58.454	9.521	.000	.359	Head
Z	σ_y	1.217	20.691	85.402	.000	.834	Head
Z	μ_x	1.512	25.699	30.701	.000	.644	Hand
R	σ_x	3.367	57.236	4.684	.004	.216	Hand
Z	σ_x	1.555	26.427	77.741	.000	.821	Hand
R	μ_y	3.091	52.547	5.221	.003	.235	Hand
R	σ_y	3.752	63.792	10.485	.000	.381	Hand
Z	σ_y	1.385	23.540	74.647	.000	.815	Hand
$R \times Z$	σ_y	5.151	87.575	4.486	.001	.209	Hand

D WOBBROCK'S ERROR MODEL

Wobbrock et al. [Wobbrock et al. 2008, 2011a] have derived a pointing error model from Fitts's law where the probability of an error P_{error} is calculated through the equation:

$$P_{\text{error}} = 1 - erf\left\{\frac{1}{A\sqrt{2}}\left[2.066 \cdot W(2^{\frac{MT_e - a'}{b'}} - 1)\right]\right\} \tag{21}$$

In the equation, $erf(\cdot)$ is the Gauss error function, A is the movement amplitude, W is the target width, a and b are empirical parameters inherited from Fitts's law, and MT_e is the *actual* time taken to reach the target. The model has shown to be useful for both 1D [Wobbrock et al. 2008] and 2D [Wobbrock et al. 2011a] pointing tasks.